J Mater Sci: Mater Med (2007) 18:1701–1709
DOI 10.1007/s10856-007-3052-3

FT-IR spectroscopy of fluoro-substituted hydroxyapatite: strengths and limitations

Llew Rintoul · Edeline Wentrup-Byrne · Shuko Suzuki · Lisbeth Grøndahl

Received: 12 October 2005 / Accepted: 26 May 2006 / Published online: 5 May 2007

Abstract Fluoro substituted hydroxyapatite (FHAp) samples were prepared by a cyclic pH method. Both calcined and uncalcined samples were subjected to elemental analysis (F, Ca, P) and X-ray diffraction (XRD) analysis to verify composition and phase purity. Good correlation between a-axis parameters and fluoride ion content was found for calcined samples, however, for uncalcined samples the fluoride ion content was higher than estimated from the a-axis values. Fourier transform infra red (FT-IR) spectroscopy analysis of the calcined samples showed OH band shifts and splitting in accordance with F-HO interactions affecting the OH vibration. We conclude that the OH libration (620–780 cm^{-1} range) is more suited for estimation of fluoride ion content than the OH stretching. In contrast, uncalcined samples all displayed FT-IR spectra similar to that of hydroxyapatite (HAp) despite the presence of fluoride ions (18–73%). FT-IR emission spectroscopy was used to probe the changes occurring in the FT-IR spectra of HAp and FHAp samples upon heating. Interpretation of the spectral changes occurring during heating to 1,000 °C and subsequent cooling is given. Room temperature spectra of samples heated to various temperatures was used to determine the temperature necessary to produce FT-IR spectra displaying the expected OH bands. A model accounting for the combined observations is proposed.

L. Rintoul · E. Wentrup-Byrne · S. Suzuki
Tissue BioRegeneration and Integration Program, Science Research Centre, Queensland University of Technology, 2 George St, GPO Box 2434, Brisbane Q 4001, Australia

L. Grøndahl (✉)
School of Molecular and Microbial Sciences, University of Queensland, St Lucia Q 4072, Australia
e-mail: l.grondahl@uq.edu.au

Introduction

Hydroxyapatite (HAp), the mineral component of bones and hard tissues in mammals, has been the subject of much research over the years, particularly in the field of biomaterials science. This is due to its importance in clinical applications involving medical devices and implants and more recently in the broad field of tissue engineering. Substitutions within the HAp lattice are observed both for naturally occurring and synthetic HAp. The most common are substitutions involving carbonate, fluoride and chloride ions for hydroxyl ions. In addition, defects can occur resulting in non-stoichiometric HAp. In the presence of fluoride ions, solid solutions of HAp and fluoroapatite (FAp) occur and these solid solutions (FHAp) have been widely studied [1]. Apatite is one of few inorganic materials that are classed as bioactive, since it supports bone ingrowth and osseointegration when used in orthopaedic, dental and maxillofacial applications. The use of HAp as a coating on orthopaedic metal implants has been shown to improve the osseointegration of the implant. However, due to the thermal instability of HAp particularly in contact with titanium, research is currently being undertaken into the use of FHAp as an alternative coating material [2, 3].

FAp belongs to the hexagonal crystal system with the space group $P6_3/m$ and with the unit cell dimensions a = 9.367(1) Å and c = 6.884(1) Å [1]. Each unit cell contains one formula unit of $Ca_{10}(PO_4)_6F_2$. If the phosphate ions are considered as spheres, then the FAp structure can be described as hexagonal close-packing of the phosphate ions with channels of octahedral holes through the structure parallel to the hexagonal c-axis; the ''X-channels''. There are two types of calcium ions in the structure; Ca(1) and Ca(2). Two thirds of the channels within the structure are occupied by Ca(1) ions which are connected

to their neighbouring calcium ions above and below by three shared oxygen atoms. In addition, each Ca(1) ion is coordinated by three more distant oxygen atoms. One third of the X-channels in the structure are occupied by fluoride ions which in turn are coordinated by three Ca(2) ions. The Ca(2) ions are seven-fold coordinated by six oxygen atoms and one fluoride ion each.

Naturally occurring HAp has a hexagonal structure similar to that of FAp. However, very pure synthetic HAp has a structure of lower symmetry, and belongs to the monoclinic crystal system, space group $P2_1/b$, with unit cell dimensions a = 9.4214(8) Å, b = 2a, c = 6.8814(7) Å, and $\gamma = 120°$ [1]. In essence, the HAp structure can be viewed as the FAp structure where fluoride ions have been substituted for the hydroxyl ions. The ''ordered column model'' predicts that the hydroxyl ions within each of the X-channels show long-range order, i.e. all hydroxyl ions are pointing in the same direction. Within individual X-channels the hydroxyl ions are arranged such that they can point in either possible direction. This explains the lower symmetry of HAp compared to FAp. Since the fluoride ion is smaller than the hydroxyl ion, the substitution of hydroxyl ions for fluoride ions results in a contraction of the unit cell dimensions, in particular the a-axis.

Detailed FT-IR spectroscopic analysis has been carried out on FHAp compounds and it has been found that, depending on the degree of substitution, the OH libration and stretching vibrations shift and split into a number of new bands [4, 5]. This has been attributed to the distribution of the fluoride and hydroxyl ions in the X-channels. This conclusion is based on evidence from the ^{19}F NMR data [6] suggesting that the hydroxyl ions neighbouring fluoride ions orient themselves in such a way that the hydrogen atoms point towards the fluoride ions. Thus, the fluoride ion forms stronger hydrogen bonds with the hydroxyl ion than the hydroxyl ion itself resulting in chain reversal in the X-channels. Correlations between the amount of fluoride ion and the position and intensity of the OH vibration bands have been found making FT-IR spectroscopy an important technique for the determination of the fluoride content in FHAp samples [4, 5]. An important point to note is that all the samples used in these studies were prepared using high temperature solid state reactions.

FT-IR has also been used to follow solid state reactions between inorganic salts. Two studies investigated the production of FHAp using HAp and either Na_2PO_3F or NH_4F as the fluoride source [7, 8]. Room temperature FT-IR spectra of the reaction mixture heated to various temperatures were used to determine the extent of the reaction. As will become clear from results presented in this paper, it is questionable whether FT-IR spectroscopy alone can be used to follow the extent of such reactions.

In the biomaterials literature there appears to be some confusion with respect to the FT-IR band assignments for FHAp samples. Spectra are often presented without making full use of the information available [9–14]. If biomaterials researchers wish to exploit FT-IR spectroscopy as a reliable analytical tool then it is essential that they recognise both the strengths and limitations of the technique.

In a recent study, we pointed out that FHAp samples prepared by solution precipitation displayed FT-IR spectra identical to hydroxyapatite despite having a high fluoride content (65%). However, a calcined sample (heated to 1,000 °C for 2 h) showed good correlation between the OH bands and the fluoride content [15]. In the present paper we have investigated a number of FHAp samples before, after and during calcination. We used IR emission spectroscopy to monitor in situ the changes in the OH band positions during heating. Combining these results with X-ray diffraction (XRD) data we postulate a model to explain the processes occurring during the heating process. In addition, we assessed the use of OH band signatures in room temperature FT-IR spectra as a means for determining the fluoride content in calcined FHAp samples.

Experimental

Synthesis of hydroxyapatite (HAp)

Calcium nitrate (11.74 g; 98.0%, Chem-Supply, Australia) dissolved in water (450 mL) was heated to 40 °C. Diammonium hydrogen phosphate (3.94 g; 98.0%, May & Baker, Australia) dissolved in water (350 mL) was slowly added to the calcium nitrate solution with vigorous stirring. The solution was brought to pH 11 by addition of concentrated ammonia (20 mL; 28.0–30.0%, Ajax Finechem, Australia). To reduce the carbonate content, the mixture was brought to the boil and immediately removed from the heat. The precipitate was aged overnight before isolation and was thoroughly washed with deionised water. The isolated product was oven dried overnight at 80 °C. The resulting HAp was ground into a fine powder using an agate mortar and pestle. A portion of this HAp was subsequently calcined at 800 °C for 1 h in air and is labelled as calc-HAp.

Synthesis of partially fluoride substituted hydroxyapatite (FHAp)

The cyclic pH variation technique described by Duff [16] was employed to incorporate fluoride ions into the HAp structure. HAp was suspended in various volumes of 0.01 M sodium fluoride (98.0%, Ajax chemicals, Australia) as listed in Table 1. The suspension was equilibrated to pH

7 overnight, after which the pH was lowered to 4 by the addition of 10 M HNO_3 (69.0–71.0%, Lab-scan, Australia) under vigorous stirring. After 30 min of equilibration, the pH was raised to 7 with 10 M NaOH (97.0%, APS, Australia). This pH cycle was repeated several times as listed in Table 1. The solid phase was filtered under mild suction, washed thoroughly with deionised water, dried overnight at 80°C, and ground into a fine powder. A portion of each sample was calcined at 800 °C (FHAp1 and 2) or 1,000 °C (FHAp4–6) for 1 h in air. These samples are referred to as calc-X, where X refers to the sample ID prior to calcination.

Elemental analysis

Samples of 10 mg were dissolved in 1 M HCl (10 mL), diluted 1:100 and subjected to calcium and phosphorous analysis on an ICPAES Spectro spectroflame P instrument using a forward power of 1,200 W, a flow rate of 1.0 mL/min and a Meinhard concentric nebuliser. Each value is an average of three 5 s integrations at 317.93 nm (Ca) or 178.29 nm (P). A fluoride selective electrode was used for fluoride analysis using citrate-hydrochloric acid buffer [17]. Samples of 10 mg were dissolved in 0.2 M HCl (20 mL) then water (10 mL) and 0.2 M trisodiumcitrate (40 mL) were added. Standard solutions were made from NaF using the same buffer system.

Vibrational spectroscopy

Infrared emission spectra were recorded on a Nicolet Nexus FT-IR (Thermo Electron, Madison, WI USA) equipped with a liquid N_2 cooled MCT detector. An emission accessory designed by Vassallo et al. [18], comprising a carbon rod furnace and an off axis paraboloidal gold mirror housed in an acrylic enclosure, was coupled to the external port of the spectrometer. The furnace was fitted with either a small Pt stub on which the sample could be placed, or a graphite stub of identical size that acted as a blackbody reference. Infrared emission was collected and directed into the interferometer via the external port by the paraboloidal mirror mounted directly above the furnace. Spectra were recorded at 50 °C intervals on heating and 100 °C intervals on cooling, from 100 to 1,000°C. Single beam measurements of the graphite and the Pt stub were obtained for each temperature. A light dusting of the sample was then placed on the Pt stub and a series of single beam measurements at each temperature were recorded. The sample was allowed to equilibrate at each temperature for a period of 5 min. Due to the low signal strength at the lower temperatures, spectra at 100 and 150°C were acquired for 1,024 scans; spectra at 200 and 250°C were acquired for 256 scans; whereas 128 scans were acquired at higher temperatures. An optical path difference (OPD) velocity of 1.8988 cm s^{-1} and a spectral resolution of 4 cm^{-1} were used throughout. Single beam emission spectra were corrected for background emission and instrumental throughput and linearised with respect to concentration using the equation [19]:

$$E = 0.5 \log[I_{bb} - I_e/(I_{bb} - I_{Pt})]$$

where I_{bb}, I_e and I_{Pt} are the intensities emitted by the graphite, the sample and the Pt stub, respectively.

Infrared absorbance spectra were obtained using a Nicolet Smart Endurance horizontal, single bounce, diamond ATR accessory on a Nicolet Nexus 870 FT-IR instrument fitted with a DTGS detector. Spectra were recorded at 4 cm^{-1} resolution for 64 scans with an OPD velocity of 0.6289 cm s^{-1}. Solids were pressed directly onto the diamond internal reflection element of the ATR accessory without further sample preparation. The FHAp-2 sample was calcined in an electrical furnace at various temperatures; 200, 300, 400, 500, 600, 700, and 800 °C at a heating rate of 100 °C/h for 1 h in air before their room temperature ATR-FT-IR spectra were recorded.

Spectral data processing was carried out using GRAMS32 software package (Galactic Industries, Salem, NH, USA).

X-ray diffraction (XRD)

Powder X-ray diffraction of all samples were performed on a PAN alytical X'Pert Pro MPD using Cu-Kα radiation generated at a voltage of 40 kV and a current of 40 mA. The divergent slit was set to 0.5° and a scatter slit at 1°. The samples were examined from 5° to 75° at a scanning speed of 0.67°/min and a step size of 0.0167°. The lattice parameters were calculated using the MDI Jade 6.5, XRD Pattern Processing, USA computer program.

Table 1 Synthesis condition for preparation of FHAp samples

Sample	Volume of 0.01 M NaF (mL/g of HAp)	Number of pH cycle
FHAp1	25	1
FHAp2	50	3
FHAp3	150	3
FHAp4	250	4
FHAp5	300	4

Results and discussion

Solid solutions of HAp and FAp were prepared by a cyclic pH method first developed by Duff [16, 20]. Such solution prepared FHAp samples displayed FT-IR spectra similar to

that of HAp (Fig. 1A–B) despite having fluoride contents in the range of 13–73% as determined by chemical analysis. The corresponding calc-FHAp samples display FT-IR spectra (Fig. 1C) that correlated with previous studies [4, 5]. This paper evaluates the use of FT-IR spectroscopy as a technique for the estimation of fluoride content in calc-FHAp. We also investigate the processes occurring during heat treatment of solution prepared FHAp materials.

Characterisation by elemental analysis and XRD

A number of FHAp samples as well as a reference sample of pure HAp were studied (Table 2). Elemental analysis generally gave values lower than the theoretical ones, but the Ca/P ratios were close to the theoretical value of 1.67, thus indicating that small amounts of impurities such as water or organic matter were present in the samples. After calcination the fluoride ion content changed only slightly (increasing by up to 5%) except for sample FHAp4 which increased from 57 to 72%. This calcined sample also displayed the largest Ca/P ratio of 1.78.

The XRD spectra indicated the presence of pure apatite with no indication of unreacted CaF_2 or coprecipitated $Ca(OH)_2$. Assuming that FHAp is a solid solution of FAp and HAp, a linear relationship between the %F and the a-axis parameter is predicted by Vergard's law. Such relationships are evident in both the solution-prepared and calcined series (Fig. 2). The values for the calcined samples agree closely with those predicted from pure HAp and FAp. This implies that for the calcined samples the substitution of fluoride ions for hydroxyl ions has occurred in the X-channels within the apatite lattice. In contrast, for the solution-prepared samples, deviation from predicted values was found. The a-axis parameter for all solution-prepared samples was larger than for their calcined counterparts (Table 2). Thus, calculation of the fluoride content using the a-axis parameter leads to an underestimation by 10–20% (Fig. 2). Some disorder such as the presence of fluoride ions within interstitial sites is probably occurring in these solution prepared samples.

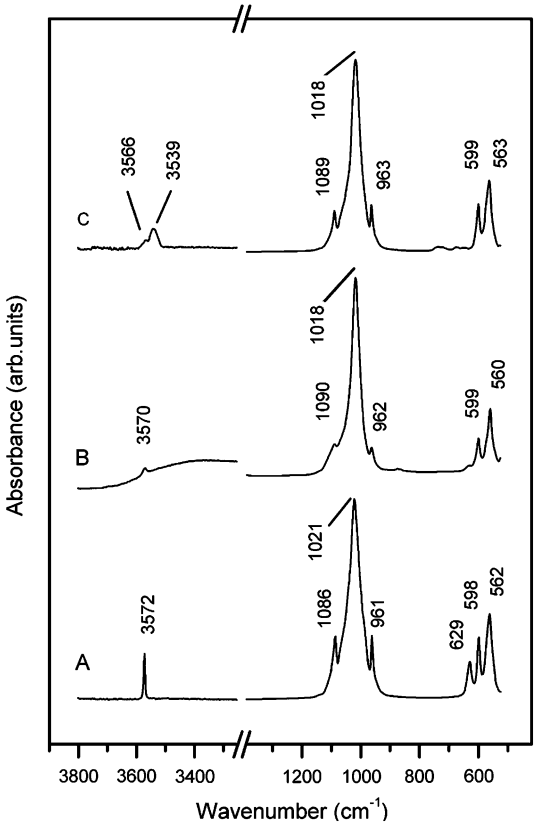

Fig. 1 ATR-FT-IR spectra of (**A**) calc-HAp, (**B**) FHAp2, and (**C**) calc-FHAp2

Use of FT-IR spectroscopy for estimation of F-content in calc-FHAp samples

The infrared spectra of all the samples studied show typical apatite phosphate modes near 1,086, 1,021, 961, 600 and 562 cm^{-1} [21]. No HPO_4^{2-} vibrations at 867 cm^{-1} [22] are observed in any of the samples. However, minor carbonate bands at 1,455, 1,423 and 875 cm^{-1} [23] are present in some samples (data not shown). The OH stretching vibration at 3,570 cm^{-1} and OH libration at 633 cm^{-1}, indicative of hydroxyapatite, is observed in HAp, calc-HAp and all FHAp samples. By contrast, in calc-FHAp samples (Fig. 1), the OH stretching and libration bands are shifted and in some cases additionally split into several bands.

According to Baumer et al. [5] the position, the number (one or two), and relative integrated absorbance of OH stretching band(s) in the 3,480–3,650 cm^{-1} region can be used to estimate the amount of fluoride ions in FHAp samples. A single band present at 3,570 cm^{-1} indicates that less than 5% of the hydroxyl ions in HAp have been substituted with fluoride ions, whereas for example, a single band at 3,538 cm^{-1} indicates that at least 75% of the hydroxyl ions have been substituted with fluoride ions. The data for our calcined samples showed similar trends to those obtained by Baumer et al. The fluoride content can be estimated from the ratio of the absorbance of the two bands, and using this approach we find that our observed values fall within the predicted ranges (Table 3).

Freund et al. investigated the position of the OH libration as a function of fluoride ion substitution into the apatite lattice [4]. Their results indicate the possibility of detecting 6–10% fluoride ion from the shift in the 631 cm^{-1} band as well as the occurrence of additional bands in the 630–750 cm^{-1} region. A schematic model giving the assignment of the OH libration bands is given in Fig. 3 [4,

Table 2 Characterisation of apatite samples

Sample	Ca/P ratio[a]	%F [b]	a-axis (Å)[c]	c-axis (Å)[c]	Other phase[c]
Hap	1.68	-	9.4239(5)	6.883(3)	
FHAp1	1.72	12.7	9.4224(9)	6.883(3)	
FHAp2	1.69	23.8	9.4137(5)	6.884(2)	
FHAp3	1.74	52.5	9.4028(6)	6.889(2)	
FHAp4	1.74	56.8	9.4009(7)	6.884(3)	
FHAp5	1.75	73.4	9.391(2)	6.885(1)	
Calc-Hap	1.71	-	9.4224(4)	6.882(2)	β-TCP (13%)
Calc-FHAp1	1.72	17.7	9.4104(4)	6.883(2)	β-TCP (14%)
Calc-FHAp2	1.71	25.8	9.4013(7)	6.8811(5)	β-TCP (10%)
Calc-FHAp3	1.74	57.9	9.3874(3)	6.8836(2)	
Calc-FHAp4	1.78	71.9	9.3786(2)	6.8849(2)	
Calc-FHAp5	1.73	73.4	9.3804(2)	6.8858(2)	

[a] Determined by ICP-AES, [b] determined by fluoride selective electrode, [c] determined by XRD

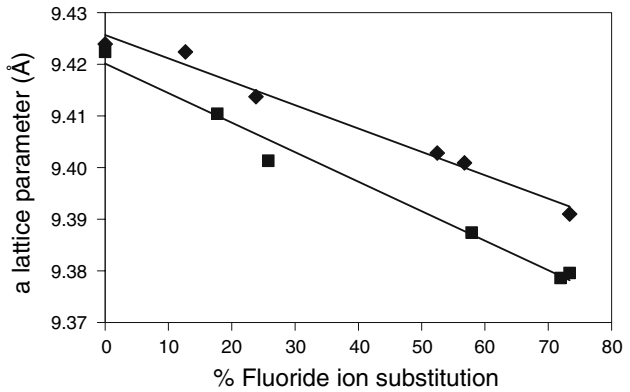

Fig. 2 Graph of a-axis parameter obtained from XRD versus %F obtained from fluoride selective electrode measurement; ■ calcined samples, ♦ un-calcined samples

24]. A number of configurations of fluoride and hydroxyl ions are possible and the model assumes that each configuration gives rise to a different vibrational band. Depending on the degree of fluoride substitution, specific configurations are more likely to predominate in the structure. By comparing the spectral features in the 800–600 cm^{-1} region of our spectra (Fig. 4) with those obtained by Freund et al. [4], the fluoride ion content of each of our samples can be estimated (Table 3). These correlate well with the experimentally obtained data. In our opinion, this spectral region lends itself far better to the estimation of the fluoride ion content in calc-FHAp samples than the 3,500–3,600 cm^{-1} region. It should be emphasised, however, that using OH bands to estimate the fluoride content requires that the samples be calcined in order to obtain meaningful results since no changes in band position or multiplicity were observed for non-calcined samples (Fig. 1).

Emission FT-IR spectroscopy

As stated above, prior to calcination solution-prepared FHAp samples displayed FT-IR spectra similar to that of HAp. The FT-IR emission technique is an alternative method for obtaining FT-IR spectra directly from samples at elevated temperatures and offers the opportunity to gain insight into the processes that take place in situ during the calcination process. At relatively low temperatures it is difficult to obtain data of sufficient signal-to-noise ratios in the high wavenumber region of the emission spectrum due to the low population of the excited state at these energies. However, by 200 °C a good signal-to-noise ratio is readily obtained.

FT-IR emission spectra of HAp in the 3,800–3,300 cm^{-1} region were obtained on heating from 100–1,000 °C and then cooling back to 100 °C. Figure 5 shows the spectra obtained at 200 °C intervals. At 200 °C the hydroxyl band at 3,568 cm^{-1}appears as a band of intermediate width, superimposed on a broad background. The background signal, which is attributable to a broad water absorption centred at 3,400 cm^{-1}, is greatly reduced by 400°C, presumably because most of the absorbed water is driven off. As a result of heating the HAp sample, a continuous shift in the ν(OH) band position to lower wavenumbers is observed (from 3,569 cm^{-1} at 100 °C to 3,552 cm^{-1} at 1,000 °C) which may be attributed to a thermally induced lattice expansion [25]. By 1,000 °C the ν(OH) of HAp has degenerated into a broad and weak band. However, on cooling the intensity of ν(OH) is regained and this suggests that the hydroxyl group becomes quite mobile above 800 °C. By 200 °C the major band shifts back to its original position, but is sharper and more distinct after calcination. This is in agreement with the observation that the

Table 3 Estimation of F-content from FT-IR spectra in calc-FHAp samples

Sample	HF/HL[a] abs	%F[b] $OH_{stretch}$	%F[c] OH_{libr}	%F[d] found
calc-Hap	–	0	0	0
calc-FHAp1	0.881	10–20	19	18
calc-FHAp2	0.528	20–25	31	26
calc-FHAp3	0.096	50–75	50	58
calc-FHAp4	0.035	50–75	76	72
calc-FHAp5	0.034	50–75	76	73

[a] ratio of high frequency (HF) and low frequency (LF) absorption of the OH stretching, [b] %fluorine predicted from the ratio of HF and LF absorption by comparing to data in reference 5, [c] %fluorine predicted from the spectral signature of the OH libration bands by comparing to data in reference 4, [d] %fluorine determined by fluoride selective electrode

a: 631 - 647 cm^{-1}

F HO **$(HO)_n$** HO:OH **$(OH)_n$** OH F

b: 713 - 720 cm^{-1}

F **HO** $(HO)_n$ HO:OH $(OH)_n$ **OH** F

c: 673 - 680 cm^{-1}

F HO $(HO)_n$ **HO:OH** $(OH)_n$ OH F

d: 747 cm^{-1}

F **HO** F

Fig. 3 Schematic illustration of the different arrangements possible along the X-columns in FHAp solid solutions and position of the corresponding infra red bands (a–d). Model adapted from Freund [4, 24]

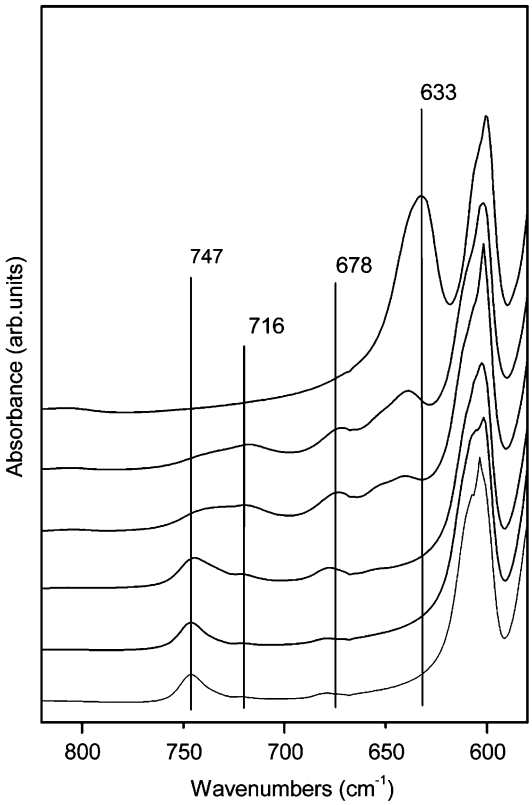

Fig. 4 ATR-FT-IR spectra of the 600–800 cm^{-1} region of (top to bottom) calc-HAp, calc-FHAp1, calcFHAp2, calc-FHAp3, calc-FHAp4, calc-FHAp5

FT-IR spectra of calcined HAp show sharper OH bands than room temperature prepared HAp [26, 27].

In the HAp emission spectra a weak shoulder is apparent at 250 °C on the low wavenumber side of the main band. This shoulder increases in intensity with increasing temperature such that by 400 °C it is clearly observed and centred at 3,533 cm^{-1} (Figure 5). The band is still present, unshifted at 600 °C, but has disappeared by 800 °C. The origin of this shoulder is not known with certainty but has been observed in previous FT-IR absorption studies of synthetic apatite at high temperatures [28, 29] as well as in dental enamel [30]. It has been proposed that the shoulder arises from hydroxyl ions that have shifted from the site occupied at room temperature to another lattice site possibly on the mirror plane [1, 28, 29]. On cooling below 600 °C the low wavenumber shoulder reappears, although as a more defined band in comparison to that obtained on heating. By 200 °C the shoulder at 3,533 cm^{-1} has virtually disappeared, although it may still be observed as an extremely weak band in the room temperature FT-IR absorption spectrum.

FHAp emission spectra in the 100–1,000 °C temperature range gave trends that were quite different from that found for HAp. A representative result, that of the FHAp2 sample, is shown in Fig. 6. Initially at 200°C, the OH stretching vibration occurs at 3,566 cm^{-1} and again is superimposed on a broad background signal from the OH stretching vibration of adsorbed water. A weak shoulder is visible at 3,537 cm^{-1}. Upon further heating the adsorbed water background vanishes (400–600°C) and the shoulder at 3,537 cm^{-1} grows in intensity corresponding to a decrease in intensity of the band at 3,566 cm^{-1}. Up to 400°C there appear to be similarities with the HAp emis-

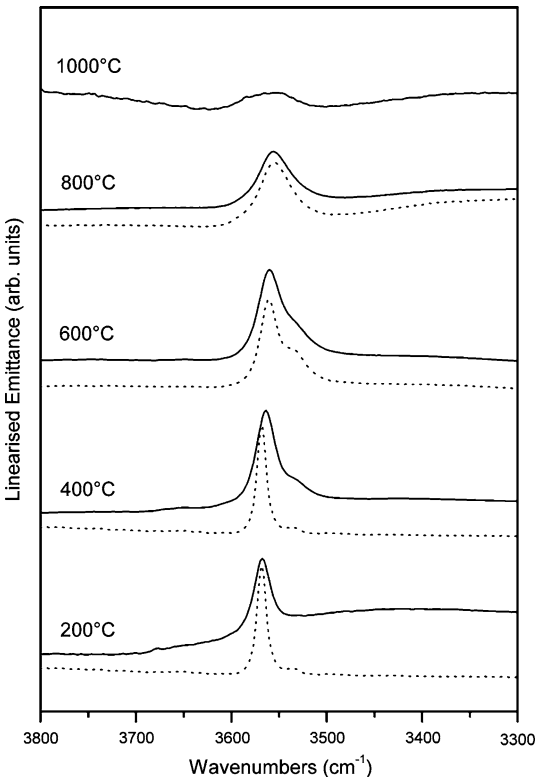

Fig. 5 Emission spectra of HAp obtained by heating from 100 °C to 1,000 °C and subsequently cooling to 100 °C. Solid lines for spectra obtained during heating; dotted lines for spectra obtained during cooling

sion spectra, although the band positions are slightly different. Of greater significance is the fact that the FHAp2 sample shows a greater relative intensity of the low wavenumber shoulder. By 600 °C it is now the major band, unlike for HAp where the low wavenumber shoulder remains the weaker band. The origin of this FHAp band is primarily attributed to the interaction of the hydroxyl ions with neighbouring fluoride ions as well as to some extend, as in HAp, to minor shifts in the hydroxyl ion lattice positions. On further heating the two bands broaden and coalesce and at the same time shift to lower wavenumbers until at 1,000 °C only a single band is visible at 3,543 cm^{-1}. The spectra of FHAp and HAp are very different during the cooling process. In the FHAp sample; the single band at 1,000°C splits into two bands as evident from 600 °C. By 400 °C, a minor band at 3,368 cm^{-1} and a major band at 3,538 cm^{-1} are clearly visible and apart from some broadening due to the elevated temperature the resulting spectrum is identical to that of the room temperature ATR FT-IR spectrum of calc-FHAp2 (Fig. 1). Due to the broadening and coalescence of the bands at 800 °C the exact temperature at which the spectrum becomes identical to that of calc-FHAp2 cannot be determined from the emission spectra, however, it is clearly above 600 °C.

Model for fluoride distribution in FHAp

Based on our observations of room temperature ATR-FT-IR and emission FT-IR spectra of FHAp samples, it is clear that changes in the position of the fluoride ions within the lattice occur during heating. The fact that the room temperature spectra of the uncalcined FHAp samples resemble that of HAp indicates that less than 5% of the hydroxyl ions have a neighbouring fluoride ion. On the other hand, the conclusion from the XRD data was that the main portion of the fluoride ions (80–90%) are most likely occupying the X-channels with a smaller portion occupying interstitial sites in the lattice. The apparent discrepancy in these observations can be explained by the following model (Fig. 7). If the fluoride ions incorporated into the structure at room temperature, sit in the lattice along the X-channels forming segments of fluoride ion chains rather than being randomly distributed among the hydroxyl ions, then only very few hydroxyl ions will have a fluoride ion as a neighbour despite large amounts of fluoride ions being present. This hypothesis is supported by findings by Pan [31] who used rotational-echo, double-resonance (Redor) NMR to study the fluoride ion distribution in a FHAp sample prepared by immersion of HAp in a NaF solution. This study revealed that the fluoride ions were not randomly distributed throughout the sample, rather, they had replaced the first two to three layers of the hydroxyl ions along the X-channels which are exposed on the surface in the a, b-plane. Furthermore, Young, Van der Lugt and Elliott [6] pointed out that the hydrogen bonding of fluoride to hydroxyl ions reduces the mobility for diffusion of a hydroxyl ion along the X-channel. Thus, it is likely that fluoride ion diffusion at room temperature is not very facile. We propose that upon heating of solution prepared FHAp samples, reorganisation of the fluoride ions within the lattice occurs leading ultimately to a random substitution. The fact that the FHAp spectrum develops over a large temperature range (independent of the heating rate) rather than as a single phase change can be attributed to the fluoride ions originating from multiple sites in the lattice. It is generally accepted that the X-channel provides the easiest diffusion path [1], and thus different temperatures will be needed for the diffusion of fluoride ions originating from different sites within the lattice which is in support of our model.

FT-IR spectra of FHAp heated to different temperatures

In order to assess the necessary temperature to which an FHAp sample must be heat treated before random distribution of fluoride ions occurs in the X-channel, a temperature series of FT-IR spectra were recorded for the FHAp2 sample. Comparison of these FT-IR spectra with that of the

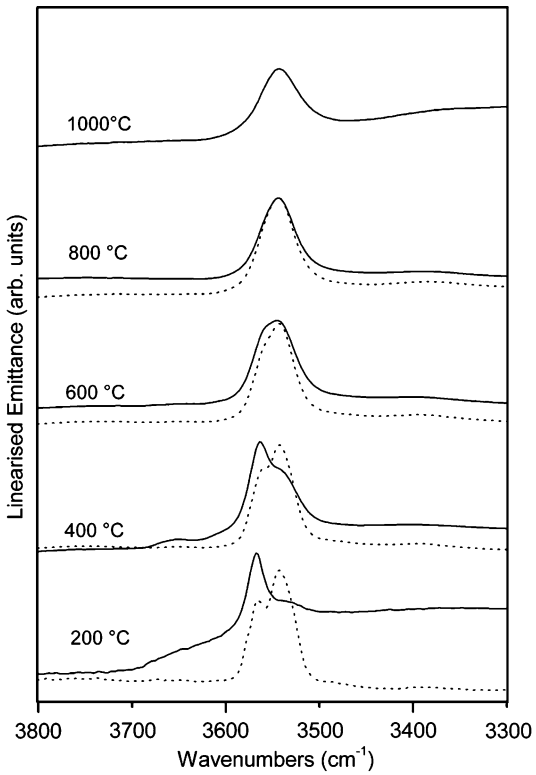

Fig. 6 Emission spectra of FHAp2 obtained by heating from 100 °C to 1,000 °C and subsequently cooling to 100 °C. Solid lines for spectra obtained during heating; dotted lines for spectra obtained during cooling

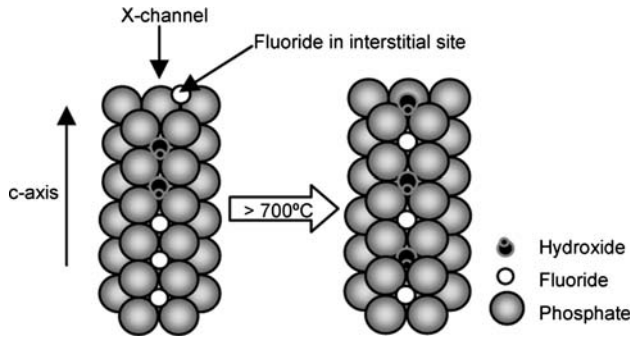

Fig. 7 Model for changes in fluoride and hydroxyl ion positions for FHAp samples during heating

calcined FHAp samples (Fig. 4) reveal that, although some changes in the spectrum have occurred at 400 °C, the spectrum at this temperature does not resemble that of calc-FHAp2. Although it is difficult to estimate the exact temperature at which the FT-IR spectrum becomes suitable for %F estimation using Freund et al. [4] and Baumer et al. [5] methods due to the bands being broad when the heat treatment was less than 800 °C; we estimate from this data that at 700 °C the band positions are identical to that of calc-FHAp2. This study confirms that the fluoride ions in the FHAp samples change positions within the lattice over a large temperature range. The results have serious implications for the use of room temperature FT-IR spectra for monitoring the degree of reaction in solid state reactions between inorganic salts which have been heated to various temperatures as has been reported previously [7, 8]. Indeed, based on our findings the conclusion is that FT-IR is an unsuitable tool to follow such reactions.

Conclusion

Our results clearly show that FT-IR spectroscopy is a powerful tool for studying FHAp samples in that it provides an accessible method for estimating the fluoride content in samples heat treated to temperatures of 800 °C or above. As demonstrated, it should, however, not be used to estimate the fluoride ion content in solution-prepared FHAp samples. Our explanation for the discrepancy in the observed FT-IR spectra of solution-prepared samples and the fluoride content is the lack of diffusion of fluoride ions in the X-channels at room temperature. In addition, the FHAp FT-IR spectrum develops over a large temperature range due to the fluoride ions originating from different positions in the lattice. The range of papers appearing in the literature where accurate analysis of FHAp samples is required means that both the strengths and the limitations of FT-IR spectroscopy as a technique must be recognised.

Acknowledgements Mr. T. Raftery, X-ray analysis facility QUT, is greatly acknowledged for XRD measurements and expert assistance in XRD analysis. Dr Wayde Martens is thanked for helpful discussions.

References

1. J. C. ELLIOTT ''Structure and chemistry of the apatites and other calcium orthophosphates'' in Studies in Inorganic Chemistry 18 (Elsevier, Amsterdam, 1994)
2. G. RIZZI, R. GROPPETTI, L. SALVARANI and A. A. SCRIVANI, *Key Eng. Mater.* 218–220 (2002) 93
3. M. WEI, J. H. EVANS and E. WENTRUP-BYRNE, *J. Australasian Ceram. Soc.* 36 (2000) 47
4. F. FREUND and R. M. KNOBEL, *J. Chem. Soc. Dalton Trans.* (1977) 1136
5. A. BAUMER, M. GANTEAUME and W. E. KLEE, *Bull. Mineral.* 108 (1985) 145
6. R. A. YOUNG, W. Van der LUGT and J. C. ELLIOTT, *Nature*, 223 (1969) 729
7. G .C. MAITI, *Ind. J. Chem.* 29A (1990) 402
8. G .C. MAITI, *Ind. J. Chem.* 31A (1992) 276
9. L. GINESTE, M. GINESTE, X. RANZ, A. ELLEFTERION, A. GUILHAM, N. ROUGUET and P. FRAYSSINET, *J. Biomed. Mater. Res. (Appl. Biomater.)* 48 (1999) 224
10. A. BIGI, E. FORESTI, A. RIPAMONTI and N. ROVERI, *J. Inorg. Biochem.* 27 (1986) 31

11. A. KRAJEWSKI, A. RAVAGLIOLI, N. ROVERI, A. BIGI and E. FORESTI, *J. Mater. Sci.* 25 (1990) 3203
12. L .J. JHA, S. M. BEST, J. C. KNOWLES, I. REHMAN, J. D. SANTOS and W. BONFIELD, *J. Mater. Sci. Mater. Med.* 8 (1997) 185
13. I. MANJUBALA, M. SIBAKUMAR and S. NAJMA NIKKATH, *J. Mater. Sci.* 36 (2001) 5481
14. H. QU and M. WEI, *J. Mater. Sci. Mater. Med.* 16 (2005) 129
15. M. WEI, J. H. EVANS, T. BOSTROM and L. GRØNDAHL, *J. Mater. Sci. Mater. Med.* 14 (2003) 311
16. E. J. DUFF, *Chem. Ind.* 8 (1974) 349
17. E. J. DUFF and J. L. STUART, *Anal. Chim. Acta* 52 (1970) 155
18. A. M. VASSALLO, P. A. COLE-CLARKE, L. S. K. PANG and A. J. PALMISANO, *Appl. Spectrosc.* 46 (1992) 73
19. L. RINTOUL, H. PANAYIOTOU, S. KOKOT, G. GEORGE, G. CASH, R. FROST, T. BUI and P. FREDERICKS, *Analyst*, 123 (1998) 571
20. E. J. DUFF, *Archs. Oral Biol.* 20 (1975) 763
21. B .O. FOWLER, *Inorg. Chem.* 13 (1974) 207
22. R.A. YOUNG and D. W. HOLCOMB, *Calcif. Tissue Int.* 34 (1982) S17
23. D .G. A. NELSON and B. E. WILLIAMSON, *Aust. J. Chem.* 35 (1982) 715
24. F. FREUND, *Inorg. Nucl. Chem. Lett.* 13 (1977) 57
25. F. FREUND, ''Ceramics and thermal transformations of minerals'', in ''The Infrared Spectra of Minerals'' edited by V. V. Farmer, Mineralogical Society, London (1974) pp. 465–482
26. H. NISHIKAWA, *Mater. Lett.* 50 (2001) 354
27. K. TÕNSUAADU, M. PELD and V. BEDER, *J. Therm. Anal. Cal.* 72 (2003) 363
28. N.W. CANT, J. A. S. BETT, R. W. GEOFFREY and W. K. HALL, *Spectrochim. Acta* 27A (1971) 425
29. I. REISNER and W. E. KLEE, *Spectrochim. Acta* 38A (1982) 899
30. J. SHI, A. KLOCKE, M. ZHANG and U. BISMAYER, *Am. Mineral.* 88 (2003) 1866
31. Y. PAN, *Phosphorous, Sulfur and Silicon* 144–146 (1999) 413